引用格式:陈修龙,蔡京成,姜帅. 一种含转动副间隙多连杆机构非线性动力学行为分析方法[J]. 山东科技大学学报(自然科学版),2019,38(2):106-116.

CHEN Xiulong,CAI Jingcheng,JIANG Shuai. Nonlinear dynamic behavior analysis of multi-linkage mechanism with clearance in revolute joint[J]. Journal of Shandong University of Science and Technology (Natural Science),2019,38(2):106-116.

一种含转动副间隙多连杆机构非线性动力学行为分析方法

陈修龙,蔡京成,姜 帅

(山东科技大学 机械电子工程学院,山东 青岛 266590)

摘 要:给出一种通过对欠驱动机构的分析来预测含转动副间隙多连杆机构动态特性的方法,利用该方法对含转动副间隙平面多连杆机构的非线性动态特性进行分析。以含转动副间隙的二自由度九连杆机构为研究对象,首先通过将转动副间隙看作虚拟无质量连杆,据此可把含转动副间隙九连杆机构变为欠驱动的十连杆机构;然后利用拉格朗日方程建立欠驱动十连杆机构的非线性动力学模型,采用龙格-库塔法对动力学模型进行数值求解,分析机构中滑块的位置、速度和加速度等运动输出、曲柄的驱动力矩等动力学响应,通过相图和庞加莱映射图对含转动副间隙的二自由度九连杆机构中存在混沌现象进行辨识;最后研究不同间隙值和不同驱动速度对九连杆机构混沌的影响,并绘制分岔图。该研究对于进一步研究含多间隙复杂连杆机构的非线性动力学研究具有重要价值。

关键词:多连杆机构; 间隙; 欠驱动机构; 混沌;分岔; 非线性动力学行为

中图分类号:TG385 **文献标志码**:A **文章编号**:1672-3767(2019)02-0106-11

DOI:10.16452/j.cnki.sdkjzk.2019.02.013

Nonlinear dynamic behavior analysis of multi-linkage mechanism with clearance in revolute joint

CHEN Xiulong,CAI Jingcheng,JIANG Shuai

(College of Mechanical and Electronic Engineering,Shandong University of Science and Technology,Qingdao,Shandong 266590,China)

Abstract: A method of forecasting the dynamic behavior of the multi-linkage mechanism with clearance by analyzing the underactuated mechanism was proposed,and the nonlinear dynamic behavior of the planar multi-linkage mechanism with clearance was studied with this method. The 2 degree of freedoms (DOFs) nine-bar mechanism with revolute clearance was taken as the research object. Firstly,by regarding the clearance of the revolute joint as a virtual massless link,the nine-bar mechanism with clearance was transformed into an underactuated ten-bar mechanism. A nonlinear dynamic model of the underactuated mechanism was established by using Lagrange equation. The Runge-Kutta method was used to solve the dynamic equations of the mechanism. The dynamic responses such as kinematics of slider,motion output of speed and acceleration speed,and driving torque of crank were analyzed. The chaos phenomenon existing in the mechanism was identified by phase diagrams and Poincaré portraits. The effects of different clearance values and different driving speeds on chaos were studied and the bifurcation diagrams were drawn. The research has an important value for the further nonlinear dynamics research of the multi-linkage mechanism with clearance.

收稿日期:2018-11-14

基金项目:山东省自然科学基金项目(ZR2017MEE066)

作者简介:陈修龙(1976—),男,河北沧州人,教授,博士生导师,主要从事机构学理论和应用技术研究. E-mail:cxldy99@163.com

Key words: multi-linkage mechanism; clearance; underactuated mechanism; chaos; bifurcation; nonlinear dynamic behavior

The planar multi-linkage mechanism is widely used in the mechanical industry for its simple manufacturing and high precision[1-2]. However, when there is a clearance between the two components of the revolute joint, it will lead to the uncertainty of the motion of the mechanism, resulting in chaos and accuracy reduction of the mechanism[3]. Therefore, it is necessary to study the nonlinear dynamic behavior of the multi-linkage mechanisms with clearance.

So far, many scholars have investigated the dynamic response of the multi-body mechanical systems with clearance. Based on the "contact-separation" model, Miedema et al. [4] divided the relative motion relationship on the revolute joint with clearance into three motion states, i. e. , contact, separation and collision, it analyzed the dynamic responses of the "contact-separation-collision" model. By considering the actual features of mechanism such as clearance, flexibility and friction, Chen et al. [5] developed a rigid-flexible model and studied the influence of the linkages flexibility and size of joint clearance on the dynamic behavior of the mechanism through automatic dynamic analysis of mechanical systems (ADAMS). With experimental platform, Erkaya et al. [6] investigated the effects of joint clearances on vibration and noise characteristics of mechanism and found that when the clearance value increases, the vibration and noise of the mechanism also become larger and exhibit nonlinear characteristics. By taking the influence of joint friction into account, Yaqubi et al. [7] analyzed the response of crank-slider mechanism with multi-clearance, and compared it with single clearance of crank-slider mechanism. Flores[8] conducted a continuous contacted force model based on the elastic Hertz theory, and analyzed the dynamic characteristics of crank-link mechanism. Yan et al. [9] used the classic impact method and the localized contact-deformation method to model contact-impact of clearance joints in the multi-body systems, and considered the effects of the gravity on the dynamic response. Zheng et al. [10] established a dynamic model of flexible multi-linkage mechanism with clearance and lubrication for ultra-precision presses, which considered the effect of revolute and spherical clearance joints, lubrication, and flexibility of crank shaft and linkage. Considering the clearance vector, Zhang et al. [11] built a collision-hinge model based on the dynamics modeling theory and analyzed the nonlinear characteristics of multi-linkage mechanism with clearances at high speed by solving the dynamic model.

Some scholars have studied the nonlinear dynamic behavior of the multi-body mechanical systems with clearance. Tang et al. [12] developed a four-bar linkage model considering clearance, and the effects of clearance value on dynamic responses were verified by Poincare map and bifurcation diagram. Muvengei et al. [13] studied the influence on dynamic behavior of clearance at different joints on the planar slider-crank mechanism without friction, and it has been found that the behavior of the mechanism changes from either periodic to chaotic, or chaotic to periodic depending on which joint has clearance. Rahmanian et al. [14] researched nonlinear dynamic behavior of a slider-crank mechanism with clearance. Bifurcation analysis has been studied with varying clearance sizes corresponding to two different crank angular velocities. Chen et al. [15] analyzed the parallel mechanism and the planar multi-linkage mechanism with clearance, which provided a reference for influence of clearance in different institutions. Wang et al. [16] described the separation process of collision by adapting a nonlinear spring damping model that conforms to the condition of contacting boundary, and discussed the nonlinear characteristics of mechanism with clearance joint. Olyaei et al. [17] studied the chaotic motion by using Poincaré map and fractal dimension of its strange attractor, and presented a control mechanism to control the chaotic motion based on the Pyragas method. From the literature view, it can be seen that there is a great need to investigate the dynamic behavior of multi-body mechanical systems with clearance, but the process of dynamic model-

ing is becoming more and more complex with the in-depth study of the mechanism with clearance. Therefore, it is imperative to find a simple and accurate analysis method to study the nonlinear dynamic behavior of multi-linkage mechanisms with clearance.

The main goal of this paper is to present a methodology to study the nonlinear dynamics behavior of a planar multi-DOFs complex mechanism with clearance and verify the effectiveness of the method by planar multi-linkage mechanism with clearance in revolute. Thus a method of forecasting the dynamic behavior of multi-linkage mechanism with clearance by analyzing the underactuated mechanism is proposed and the nonlinear dynamic behavior of 2 DOFs nine-bar mechanism with a revolute clearance is studied. The dynamic model of the underactuated mechanism is established and the motion characteristic of slider and driving torque of crank are studied. The chaos phenomenon existing in the mechanism is identified by phase diagrams, Poincaré portraits, and bifurcation diagrams. The effect of different clearance values and driving speeds on chaos are analyzed.

1 Establishment of dynamic model of mechanism with clearance

1.1 Model transformation of planar nine-bar mechanism with a revolute clearance

The mechanism consists of frame, Crank 1, Link 2, Link 3, Crank 4, Rocking-bar 6, Link 7, Link 8 and Slider 9. Link 5 is part of the frame. The model diagram of planar nine-bar mechanism with clearance is shown in Fig. 1. In the model, the clearance revolute joint between Link 3 and Crank 4 is replaced by virtual massless link, which is called the clearance bar r. The DOF of the mechanism has changed to 3, larger than the number of driving. The model is transformed from the multi-linkage mechanism with clearance to the underactuated mechanism.

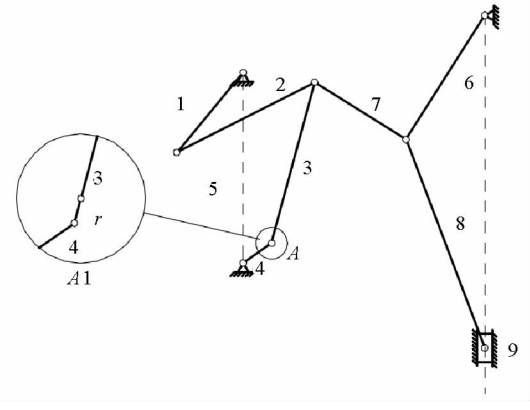

Fig. 1 Model diagram of nine-bar linkage mechanism with a revolute clearance

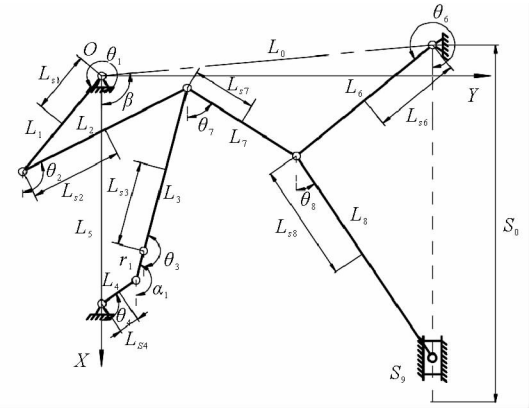

Fig. 2 Coordinate system of the mechanism with a revolute clearance

1.2 Establishment of kinematics equation with a revolute clearance

The mechanism in the coordinate system is shown in Fig. 2. It is supposed that the length of Crank 1 is L_1 ,and its angle is θ_1 (the angle between the rod vector and the X axis in the positive direction counter anti-clockwise), its vector is $\overrightarrow{L_1}$. The other bars in the mechanism are also expressed in the same way, forming closed vector polygons consisting of vector bars. In this polygon, the sum of vectors must be zero.

For the transformed mechanism, the closed vector equation can be expressed as

$$\begin{cases} L_1\cos\theta_1 + L_2\cos\theta_2 = L_3\cos\theta_3 + r_1\cos\alpha_1 + L_4\cos\theta_4 + L_5, \\ L_1\sin\theta_1 + L_2\sin\theta_2 = L_3\sin\theta_3 + r_1\sin\alpha_1 + L_4\sin\theta_4, \\ L_1\cos\theta_1 + L_2\cos\theta_2 = L_6\cos\theta_6 + r_2\cos\beta + L_7\cos\theta_7, \\ L_1\sin\theta_1 + L_2\sin\theta_2 = L_6\sin\theta_6 + r_2\sin\beta + L_7\sin\theta_7, \\ L_6\cos\theta_6 + L_8\cos\theta_8 + S_9 = S_0, \\ L_6\sin\theta_6 + L_8\sin\theta_6 = 0. \end{cases} \tag{1}$$

In the above model, the length of each bar and the motion law of the driving link are known, so six direction angles θ_2, θ_3, θ_5, θ_6, θ_7, θ_8 are unknown, and the clearance angle α_1 and the position of the slider S_9 can be obtained by the above equation.

1.3 Establishment of dynamic equation with a revolute clearance

The dynamic model of the mechanism with clearance established by Lagrange equation is expressed as

$$\frac{\mathrm{d}}{\mathrm{d}t}\left(\frac{\partial E}{\partial \dot{q}_i}\right) - \frac{\partial E}{\partial q_i} + \frac{\partial V}{\partial q_i} = Q_i, i = 1, 2, 3. \tag{2}$$

Where, E, V, Q_i, q_i represent kinetic energy, potential energy, general force and generalized coordinates respectively, and $q_1 = \theta_1$, $q_2 = \theta_4$, $q_3 = \alpha_1$.

The equation of the kinetic energy of the mechanism can be written as

$$E = \frac{1}{2}\sum_{\substack{i=1 \\ i\neq 1,4,5,6}}^{9} m_i v_{si}^2 + \frac{1}{2}\sum_{\substack{i=1 \\ i\neq 5,9}}^{9} J_i \dot{\theta}_i^2 . \tag{3}$$

Where, m_i represents the mass of components, v_{si} corresponds to the velocity of the centroid of component i, J_i corresponds to the moment of inertia of the component i, $\dot{\theta}_i$ corresponds to the angular velocity of the component i.

When the O point is zero potential energy position and the X direction is the gravitational direction, the potential energy of the mechanism can be written as

$$V = \sum_{\substack{i=1 \\ i\neq 5}}^{9} -m_i g x_{si} . \tag{4}$$

Considering the principle of virtual work, the relationship between generalized force and virtual displacement can be expressed as

$$\delta W = Q_1\delta q_1 + Q_2\delta q_2 + Q_3\delta q_3 . \tag{5}$$

Where Q_1, Q_2 and Q_3 represent generalized force, respectively.

For the mechanism with clearance, the equation based on the virtual work principle is given by

$$\delta W = Q_1\delta q_1 + Q_2\delta q_2 = M_1\delta q_1 + M_2\delta q_2 - F_r\left(\frac{\partial(S_0 - S_9)}{\partial q_1}\delta q_1 + \frac{\partial(S_0 - S_9)}{\partial q_2}\delta q_2\right). \tag{6}$$

According to Eq. (6), the generalized force of the non-conservative system can be written as

$$\begin{bmatrix} Q_1 \\ Q_2 \\ Q_3 \end{bmatrix} = \begin{bmatrix} M_1 + F_r\dfrac{\partial S_9}{\partial q_1} \\ M_2 + F_r\dfrac{\partial S_9}{\partial q_2} \\ 0 \end{bmatrix} . \tag{7}$$

Where, M_1 and M_2 represent the driving torques of Crank 1 and Crank 4 respectively, and F_r is the resistance of slider.

1.4 Solution of the kinematic differential equation of the model

According to Eqs. (2), (3), (4) and (7), the Lagrange equation can be transformed as

$$\begin{cases} Q_1 = \ddot{q}_1 J_{11} + \ddot{q}_2 J_{12} + \ddot{q}_3 J_{13} + \frac{1}{2}\dot{q}_1^2 \frac{\partial J_{11}}{\partial q_1} + \dot{q}_1\dot{q}_2 \frac{\partial J_{11}}{\partial q_2} + \dot{q}_1\dot{q}_3 \frac{\partial J_{11}}{\partial q_3} + (\frac{\partial J_{12}}{\partial q_3} + \frac{\partial J_{13}}{\partial q_2} - \frac{\partial J_{33}}{\partial q_1})\dot{q}_2\dot{q}_3 \\ \quad + (\frac{\partial J_{12}}{\partial q_2} - \frac{1}{2}\frac{\partial J_{22}}{\partial q_1})\dot{q}_2^2 + (\frac{\partial J_{13}}{\partial q_3} - \frac{1}{2}\frac{\partial J_{33}}{\partial q_1})\dot{q}_3^2 + \frac{\partial V}{\partial q_1}, \\ Q_2 = \ddot{q}_1 J_{12} + \ddot{q}_2 J_{22} + \ddot{q}_3 J_{23} + \dot{q}_1\dot{q}_2 \frac{\partial J_{22}}{\partial q_1} + \frac{1}{2}\dot{q}_2^2 \frac{\partial J_{22}}{\partial q_2} + \dot{q}_2\dot{q}_3 \frac{\partial J_{22}}{\partial q_3} + (\frac{\partial J_{12}}{\partial q_1} - \frac{1}{2}\frac{\partial J_{11}}{\partial q_2})\dot{q}_1^2 \\ \quad + (\frac{\partial J_{12}}{\partial q_3} + \frac{\partial J_{23}}{\partial q_1} - \frac{\partial J_{13}}{\partial q_2})\dot{q}_1\dot{q}_3 + (\frac{\partial J_{23}}{\partial q_3} - \frac{1}{2}\frac{\partial J_{33}}{\partial q_2})\dot{q}_3^2 + \frac{\partial V}{\partial q_2}, \\ Q_3 = \ddot{q}_1 J_{13} + \ddot{q}_2 J_{23} + \ddot{q}_3 J_{33} + \dot{q}_1\dot{q}_3 \frac{\partial J_{33}}{\partial q_1} + \dot{q}_2\dot{q}_3 \frac{\partial J_{33}}{\partial q_2} + \frac{1}{2}\dot{q}_3^2 \frac{\partial J_{33}}{\partial q_3} + (\frac{\partial J_{13}}{\partial q_1} - \frac{1}{2}\frac{\partial J_{11}}{\partial q_3})\dot{q}_1^2 \\ \quad + (\frac{\partial J_{13}}{\partial q_2} + \frac{\partial J_{23}}{\partial q_1} - \frac{\partial J_{12}}{\partial q_3})\dot{q}_1\dot{q}_2 + (\frac{\partial J_{23}}{\partial q_2} - \frac{1}{2}\frac{\partial J_{22}}{\partial q_3})\dot{q}_3^2 + \frac{\partial V}{\partial q_3}. \end{cases} \tag{8}$$

Because the generalized force corresponding to the clearance bar is zero($Q_3 = 0$), the second-order nonlinear differential equations is derived for q_3 . Then

$$\ddot{q}_3 = f(q_1, q_2, q_3, \dot{q}_1, \dot{q}_2, \dot{q}_3) . \tag{9}$$

Eq. (9) can be expressed as

$$\ddot{q}_3 = A_0 + A_{11}\dot{q}_1^2 + A_{22}\dot{q}_2^2 + A_{33}\dot{q}_3^2 + A_{12}\dot{q}_1\dot{q}_2 + A_{13}\dot{q}_1\dot{q}_3 + A_{23}\dot{q}_2\dot{q}_3. \tag{10}$$

Where, $A_0 = J_{13}\ddot{q}_1 + J_{23}\ddot{q}_2 + \frac{\partial V}{\partial q_3}$, $A_{11} = (\frac{\partial J_{13}}{\partial q_1} - \frac{1}{2}\frac{\partial J_{11}}{\partial q_3})/J_{33}$, $A_{22} = (\frac{\partial J_{23}}{\partial q_2} - \frac{1}{2}\frac{\partial J_{22}}{\partial q_3})/J_{33}$, $A_{33} = \frac{1}{2}\frac{\partial J_{11}}{\partial q_3 J_{33}}$, $A_{12} = (\frac{\partial J_{13}}{\partial q_2} + \frac{\partial J_{23}}{\partial q_1} - \frac{\partial J_{12}}{\partial q_3})/J_{33}$, $A_{13} = \frac{\partial J_{33}}{\partial q_1 J_{33}}$, $A_{23} = \frac{\partial J_{33}}{\partial q_2 J_{33}}$.

The fourth order Runge-Kutta is used to solve Eq. (11), and the value of the unknown quantity α_1 can be obtained. Then, the α_1 is brought into Eq. (2), and the displacement, velocity and acceleration of the slider can be deduced.

With the value of α_1 being known, the expressions of two driving torques can be derived from Eq. (7) and Eq. (8). Then

$$\begin{cases} M_1 = \ddot{q}_1 J_{11} + \ddot{q}_2 J_{12} + \ddot{q}_3 J_{13} + \frac{1}{2}\dot{q}_1^2 \frac{\partial J_{11}}{\partial q_1} + \dot{q}_1\dot{q}_2 \frac{\partial J_{11}}{\partial q_2} + \dot{q}_1\dot{q}_3 \frac{\partial J_{11}}{\partial q_3} + (\frac{\partial J_{12}}{\partial q_3} + \frac{\partial J_{13}}{\partial q_2} - \frac{\partial J_{33}}{\partial q_1})\dot{q}_2\dot{q}_3 \\ \quad + (\frac{\partial J_{12}}{\partial q_2} - \frac{1}{2}\frac{\partial J_{22}}{\partial q_1})\dot{q}_2^2 + (\frac{\partial J_{13}}{\partial q_3} - \frac{1}{2}\frac{\partial J_{33}}{\partial q_1})\dot{q}_3^2 + \frac{\partial V}{\partial q_1} - F_r\frac{\partial S_9}{\partial q_1}, \\ M_2 = \ddot{q}_1 J_{12} + \ddot{q}_2 J_{22} + \ddot{q}_3 J_{23} + \dot{q}_1\dot{q}_2 \frac{\partial J_{22}}{\partial q_1} + \frac{1}{2}\dot{q}_2^2 \frac{\partial J_{22}}{\partial q_2} + \dot{q}_2\dot{q}_3 \frac{\partial J_{22}}{\partial q_3} + (\frac{\partial J_{12}}{\partial q_1} - \frac{1}{2}\frac{\partial J_{11}}{\partial q_2})\dot{q}_1^2 \\ \quad + (\frac{\partial J_{12}}{\partial q_3} + \frac{\partial J_{23}}{\partial q_1} - \frac{\partial J_{13}}{\partial q_2})\dot{q}_1\dot{q}_3 + (\frac{\partial J_{23}}{\partial q_3} - \frac{1}{2}\frac{\partial J_{33}}{\partial q_2})\dot{q}_3^2 + \frac{\partial V}{\partial q_2} - F_r\frac{\partial S_9}{\partial q_2}. \end{cases} \tag{11}$$

2 Nonlinear characteristics of planar nine-bar mechanism with a revolute clearance

2.1 Parameter setting of the mechanism with a revolute clearance

System parameters of the mechanism with clearance can be seen in Tab. 1.

2.2 Chaos identification of mechanism with a revolute clearance

The speed of Crank 1 and Crank 4 are set to $-\pi$ rad/s and π rad/s respectively, the length of the clearance bar is 0.15 mm.

The kinematic characteristic of slider are shown from Fig. 3 to Fig. 8. The displacement and displacement error are shown in Fig. 3 and Fig. 4 respectively. From Fig. 3 and Fig. 4, it can be seen that the displacement curve of the slider with a revolute clearance basically conforms to the displacement curve of the slider in the ideal state, and the maximum displacement error of the slider appears in the 1.232 s, and the

error value is 7.806×10^{-5} m.

Tab. 1 Dimensions and mass properties for the 2 DOFs nine-bar mechanism

Component	Crank 1	Link 2	Link 3	Crank 4	Link 5	Link 6
Length/m	L_1	L_2	L_3	L_4	L_5	L_6
	0.300	0.893	0.962	0.100	1.100	0.850
	L_{31}	L_{32}	L_{33}	L_{34}	L_{35}	L_{36}
	0.150	0.446	0.481	0.050	—	0.425
Mass/kg	0.985	2.836	3.051	0.361	—	2.701
Moment of inertia/(kg·m^2)	8.390×10^{-3}	1.957×10^{-1}	2.437×10^{-1}	4.774×10^{-4}	—	1.693×10^{-1}

Component	Link 7	Link 8	Slider 9
Length/m	L_7	L_8	
	0.623	0.850	
	L_{S7}	L_{S8}	—
	0.312	0.425	
Mass/kg	1.993	2.701	4.288
Moment of inertia/(kg·m^2)	6.818×10^{-2}	1.693×10^{-1}	—

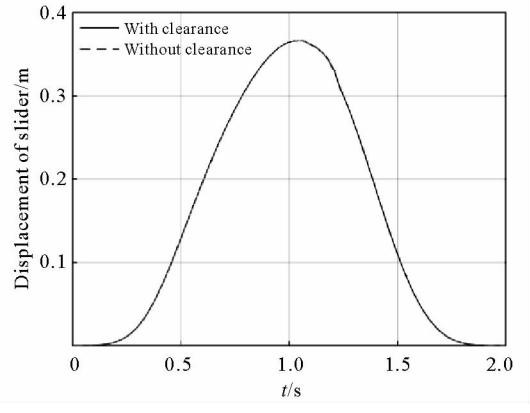

Fig. 3 Displacement of slider

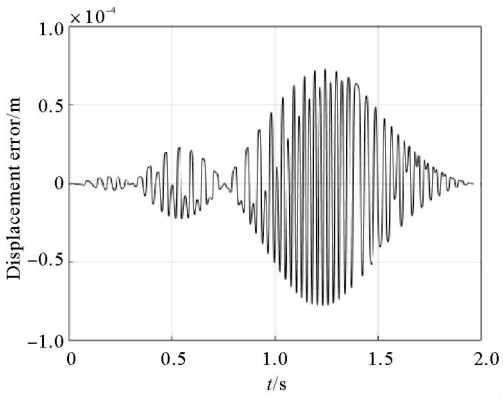

Fig. 4 Displacement error of slider

The velocity and velocity error of the slider are shown in Fig. 5 and Fig. 6 respectively, and the results show that the clearance has a definite effect on the speed of the slider. The maximum velocity error of the slider appears in the 1.187 s, and the error value is 0.029 m/s.

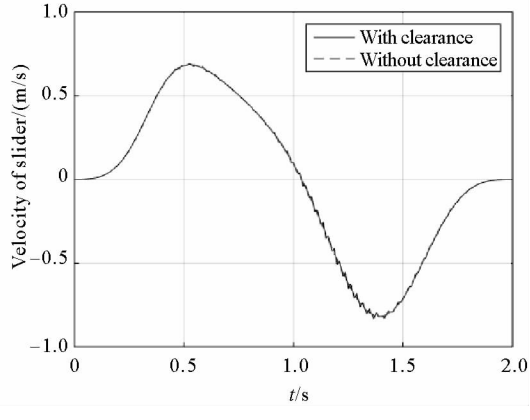

Fig. 5 Velocity of slider

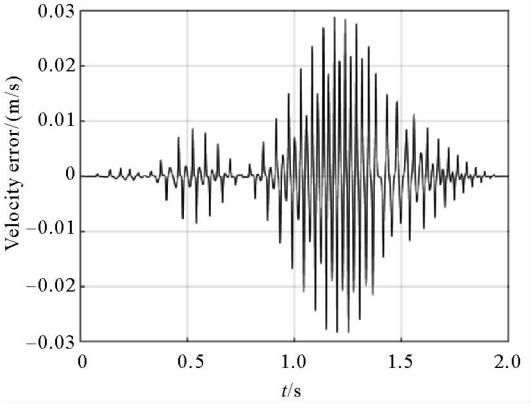

Fig. 6 Velocity error of slider

The acceleration and acceleration error of the slider are shown in Fig. 7 and Fig. 8 respectively. From Fig. 7 and Fig. 8, it can be seen that the clearance has a more obvious influence on the acceleration, and that the acceleration curve fluctuates violently and a great peak occurs. The maximum acceleration error of the slider appears in the 1.152 s, and the error value is 8.684 m/s^2.

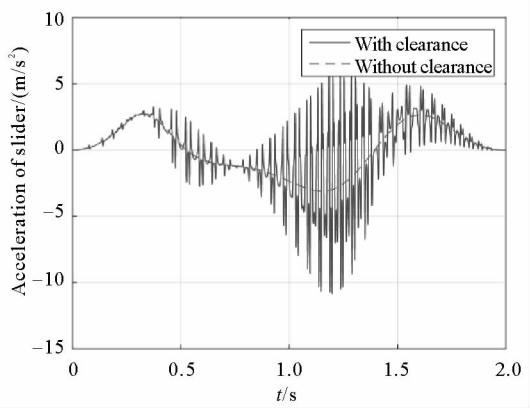

Fig. 7 Acceleration of slider

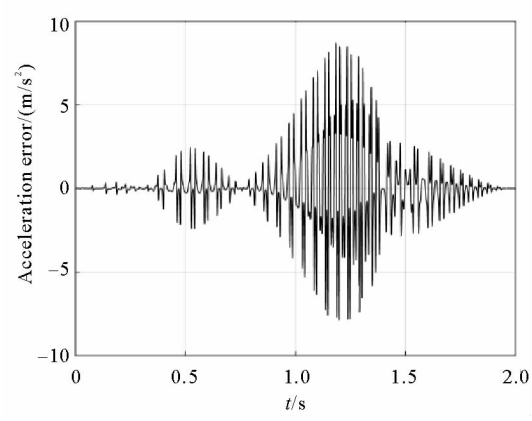

Fig. 8 Acceleration error of slider

The driving torque curves of Crank 1 and Crank 4 are shown in Fig. 9 (a) and 9 (b) respectively. From Fig. 9, it can be seen that the driving torques of Crank 1 and Crank 4 generate peak values that are all at 0.528 s, the peak values are 43.394 N · m and 11.576 N · m respectively. The results show that the existence of clearance has a greater influence on the driving torque of the mechanism, which will cause obvious oscillation of the driving torque.

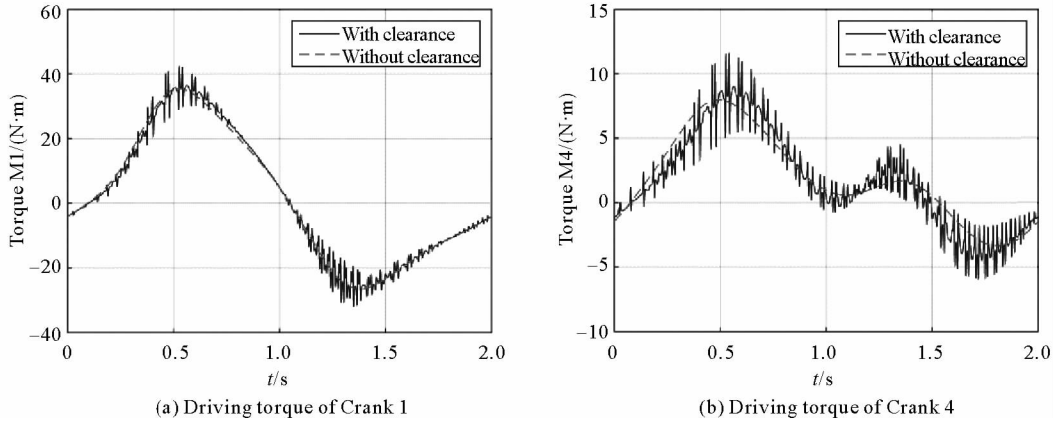

Fig. 9 Driving torque of Crank

By drawing the phase diagrams and Poincaré portraits of the clearance bar, the chaotic phenomena in the motion of the mechanism are identified.

The phase diagram of the mechanism with clearance is shown in Fig. 10. It can be seen from Fig. 10 that the trajectory of the curve is not closed and in a mess, and the general trend of the phase diagram is more chaos, so the mechanism is in a chaotic state.

The Poincaré portraits is to cross the trajectory of the continuous motion with one plane, then the state of the motion can be judged succinctly according to the condition that the trajectory passes through the

cross section. When the Poincaré cross section has only one isolated Poincaré mapping point or very few discrete points, the motion of the system is the periodic motion. When a continuous or discrete closed curve appears on the Poincaré cross section, the system does the quasi-periodic motion. When the Poincaré cross section has some patchy distribution of point set, the system is in chaotic state.

Poincaré portraits of the mechanism with clearance are shown in Fig. 11. It can be seen from Fig. 11 that the mapping points on the Poincaré cross section are distributed irregularly, indicating that the mechanism is in a chaotic state.

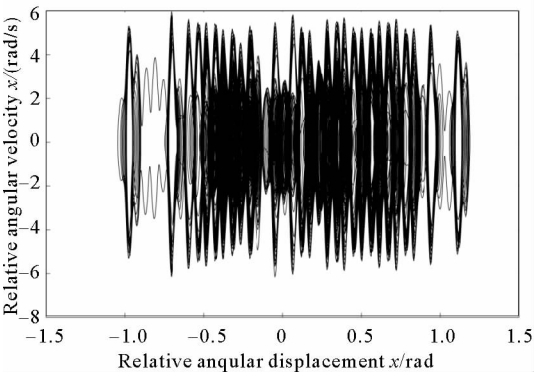

Fig. 10 Phase diagram of the underactuated mechanism

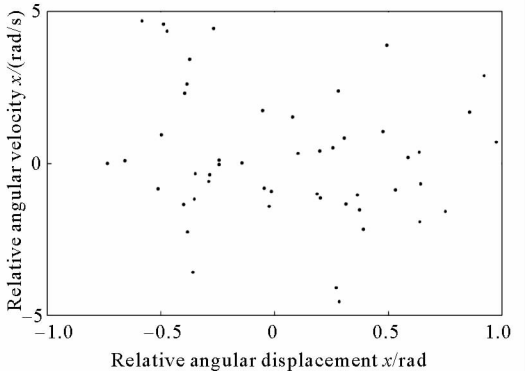

Fig. 11 Poincaré portraits of the underactuated mechanism

2.3 The effect of main parameters of the mechanism on the chaotic motions

2.3.1 Effect of clearance value on chaotic motion

To study the effect of clearance value on mechanism chaos, The driving speeds of Crank 1 and Crank 4 are fixed value $-\pi$ rad/s and π rad/s respectively. The changes of the mechanism are observed by changing the length of the clearance bar.

The Poincaré portraits of the mechanism with different clearance values are shown in Fig. 12. The Poincaré portraits of Fig. 12(a), (b), (c) and (d) correspond to four sets of values $r1$ of 0.05, 0.10, 0.15 and 0.25 mm respectively. When $r1$ is 0.05 mm, the mapping points in the Poincaré portrait are chaotic and irregular, showing that the mechanism is already in chaos. With the increase of the length of the clearance bar, the distribution of Poincaré mapping points gradually decreases, but it is always in chaos. As shown in this model, even a small clearance will lead to chaos, and the intensity of chaos will decrease with the increase of the length of the clearance bar.

In the study of chaos, bifurcations can clearly reflect the effects of different variables on system behavior. So the bifurcation diagram of relative angular velocity versus clearance values is drawn to better realize the relationship between them. The lengths of the clearance bar ranging from 0.01 to 0.5 mm are selected to research bifurcation phenomena, as shown in Fig. 13. According to the bifurcation diagram, the same conclusion can be obtained as the Poincaré portraits. Even a small clearance will lead to chaos, and the intensity of chaos will decrease with the increase of the length of the clearance bar. Through analysis, the reason for this phenomenon may be that the longer the gap bar is, the lower the swing frequency is.

2.3.2 Effect of driving speed of two cranks on chaotic motion

In analyzing the effect of the driving speed of two cranks on chaotic motion, the length of the clearance bar is set to the fixed value of 0.15 mm, and the changes of the mechanism are observed by changing the driving speed of two cranks. The unit of driving speed is 'rad/s', and it is omitted in the following text.

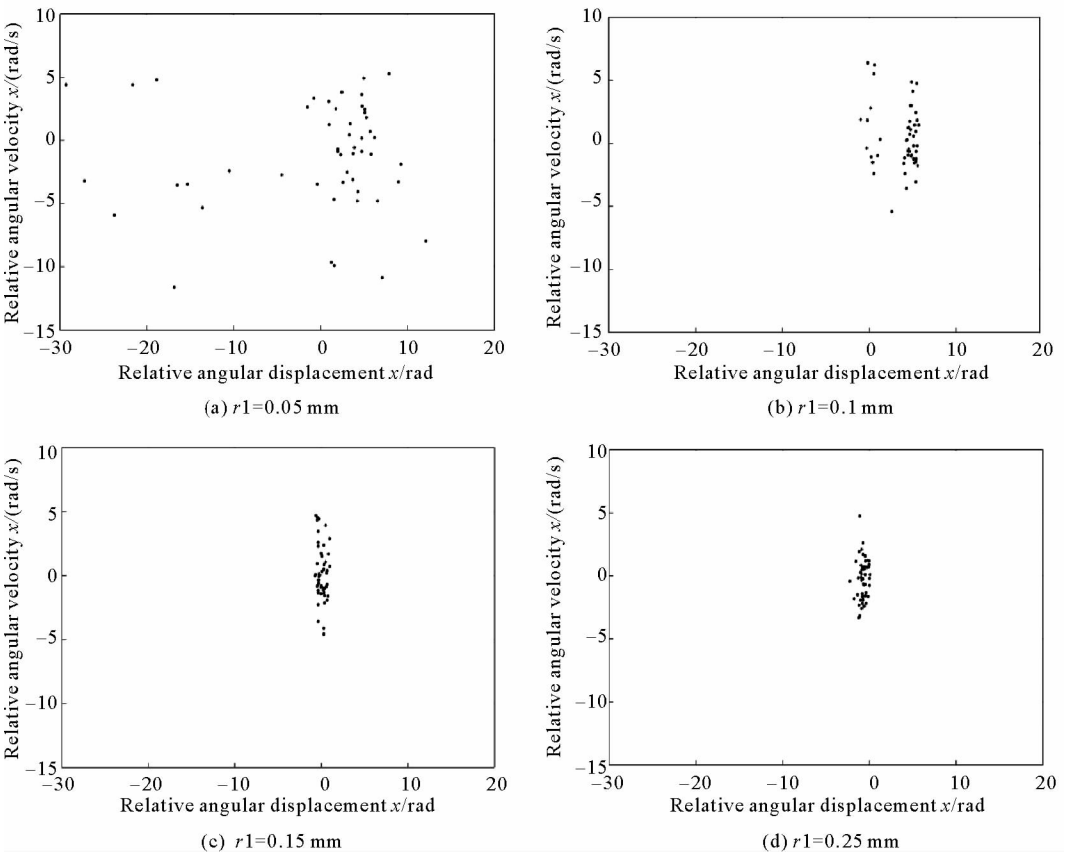

Fig. 12 Poincaré portrait of the underactuated mechanism for different lengths of the clearance bar

The Poincaré portraits of the underactuated mechanism with different driving speeds are shown in Fig. 14. The Poincaré portraits of Fig. 14(a),(b),(c) and (d) correspond to four sets of different driving speeds $\omega_1 = -0.5\pi, \omega_4 = 0.5\pi$, $\omega_1 = -\pi, \omega_4 = \pi, \omega_1 = -1.5\pi, \omega_4 = 1.5\pi$ and $\omega_1 = -2.5\pi, \omega_4 = 2.5\pi$. As is shown in Fig.14(a), the mechanism is in a chaotic state. By comparing with other Poincaré portraits, it can be seen that the chaos is more obvious with the increase of the driving speed.

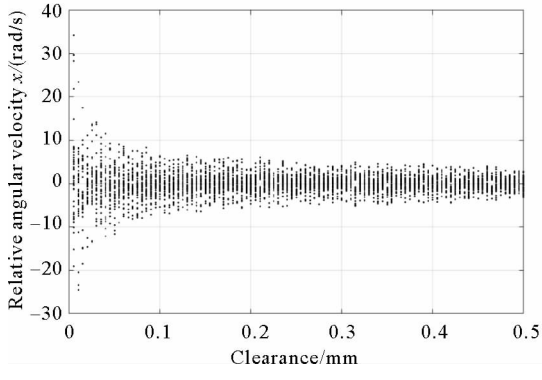

Fig. 13 Bifurcation diagram with varying clearance

Bifurcation diagram with varying driving speeds is shown in Fig. 15. The variation range of driving speeds of Crank 1 and Crank 4 are $[-0.05\pi, -5\pi]$ and $[0.05\pi, 5\pi]$ respectively. From Fig. 15, when the driving speed is small, the chaos of the mechanism is not so obvious. With the increase of the driving speed, the bifurcation diagram presents a divergence trend, and the chaotic phenomenon is more obvious. The main reason is that with the increase of the driving speed, the vibration of the mechanism becomes more intense. On the whole, the driving speed has great influence on the motion state of the mechanism.

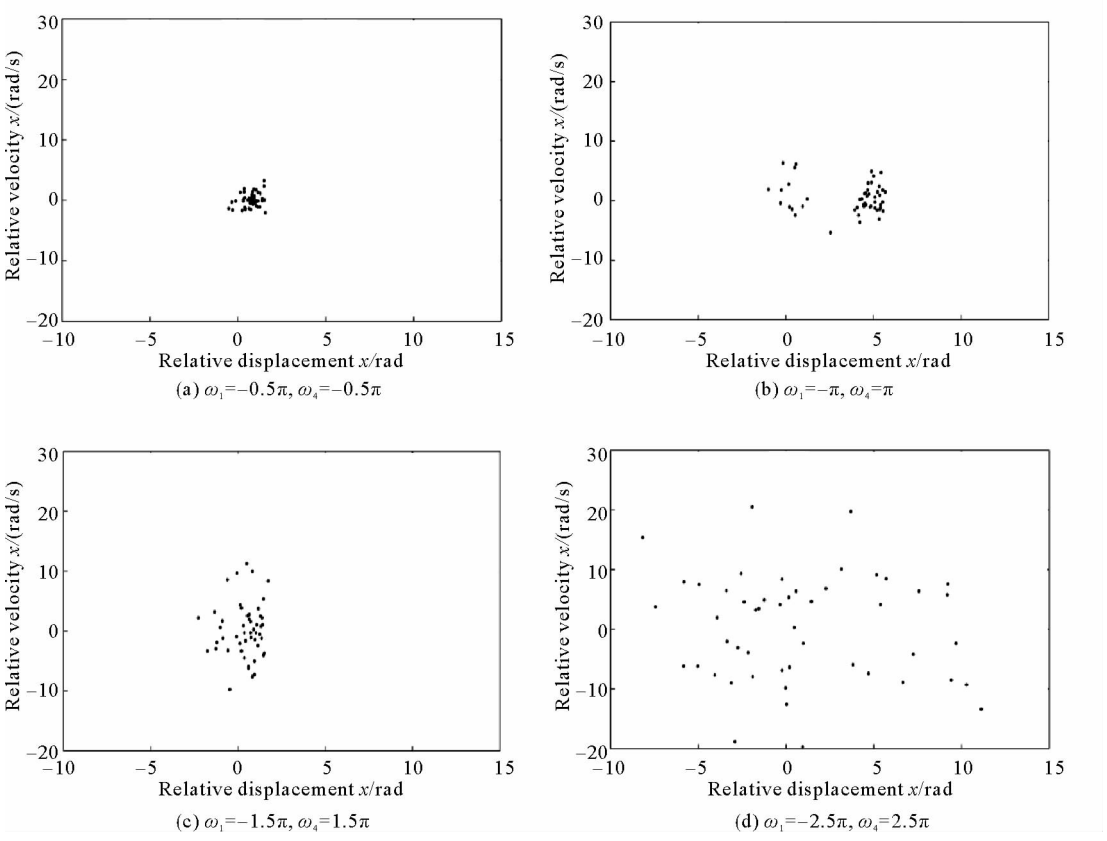

Fig. 14 Poincaré portrait of the mechanism with clearance for different driving speeds

3 Conclusions

In this paper, the nonlinear dynamic behavior of a planar 2 DOFs nine-bar mechanism with clearance is analyzed, the following conclusions can be drawn:

1) A method of forecasting the dynamic behavior of multi-linkage mechanism with clearance by analyzing the underactuated mechanism is proposed. And the dynamic equation of the mechanism with clearance is established according to the Lagrange equation.

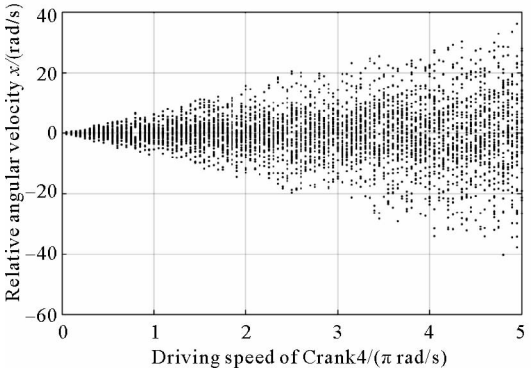

Fig. 15 Bifurcation diagram with varying driving speeds of two Cranks

2) The solution of the nonlinear dynamic model of the mechanism with clearance is realized by Runge-Kutta method. The kinematic characteristics of slider and the driving torque of the crank are analyzed. The nonlinear characteristics of the mechanism are obtained by the phase diagram and Poincaré portraits, and it is found that the clearance has an obvious effect on the stability of the mechanism and will cause chaos.

3) The effects of different clearance values and different driving speeds on the nonlinear characteristics of clearance mechanism are studied. Bifurcation diagrams with varying clearance values and driving speeds are drawn. The results show that with the increase of the length of the clearance bar, the chaos of the mechanism decreases gradually, and the chaotic phenomenon of the mechanism becomes more obvious, as the driving speed increases.

4) Through the above steps, the feasibility of the proposed method for analyzing the nonlinear characteristics of the multi-linkage mechanism with clearance is verified.

Reference:

[1]GE X F, ZHU C A, JIN Y. Optimization design for a new large-scale eight-link mechanical press[J]. Journal of Mechanical Science and Technology, 2014, 28(4): 1403-1410.

[2]CHEN X L, GAO W H, JIANG S, et al. Static and dynamic analysis of a novel single-DOF six bar mechanical press mechanism[J]. Journal of Shandong University of Science and Technology (Natural Science), 2017, 36(5): 80-90.

[3]YAQUBI S, DARDEL M, DANIALI H M, et al. Modeling and control of crank-slider mechanism with multiple clearance joints[J]. Multibody System Dynamics, 2016, 36(2): 143-167.

[4]MIEDEMA B, MANSOUR W M. Mechanical joints with clearance: A three-mode model[J]. Journal of Engineering for Industry, 1976, 98(4): 1319.

[5]CHEN Y, SUN Y, CHEN C. Dynamic analysis of a planar slider-crank mechanism with clearance for a high speed and heavy load press system[J]. Mechanism & Machine Theory, 2016, 98: 81-100.

[6]ERKAYA S, UZMAYĪ. Experimental investigation of joint clearance effects on the dynamics of a slider-crank mechanism [J]. Multibody System Dynamics, 2010, 24(1): 81-102.

[7]YAQUBI S, DARDEL M, DANIALI H M, et al. Modeling and control of crank-slider mechanism with multiple clearance joints[J]. Multibody System Dynamics, 2016, 36(2): 1-25.

[8]FLORES P. A parametric study on the dynamic response of planar multibody systems with multiple clearance joints[J]. Nonlinear Dynamics, 2010, 61: 633-653.

[9]SUN Y, LI C, LIU J, et al. Dynamic modeling of multibody system with clearance joints[J]. Journal of Vibration Engineering, 2003, 16(3): 290-294.

[10]ZHENG E L, ZHU R, ZHU S H, et al. A study on dynamics of flexible multi-link mechanism including joints with clearance and lubrication for ultra-precision presses[J]. Nonlinear Dynamics, 2016, 83(1/2): 137-159.

[11]ZHANG Z L, WU S J, ZHAO W Q, et al. Dynamic characteristics of high-speed multi-link transmission mechanisms with clearance[J]. Journal of Vibration & Shock, 2014, 33(14): 66-71.

[12]TANG Y G, CHANG Z Y, DONG X G, et al. Nonlinear dynamics and analysis of a four-bar linkage with clearance[J]. Frontiers of Mechanical Engineering, 2013, 8(2): 160-168.

[13]MUVENGEI O, KIHIU J, IKUA B. Numerical study of parametric effects on the dynamic response of planar multi-body systems with differently located frictionless revolute clearance joints[J]. Mechanism & Machine Theory, 2012, 53(7): 30-49.

[14]RAHMANIAN S, GHAZAVI M R. Bifurcation in planar slider-crank mechanism with revolute clearance joint[J]. Mechanism & Machine Theory, 2015, 91(19): 86-101.

[15]CHEN X L, JIANG S, DENG Y, et al. Dynamics analysis of 2-DOF complex planar mechanical system with joint clearance and flexible links[J]. Nonlinear Dynamics, 2018(1): 1-26.

[16]WANG G Q, LIU H Z, HE C A. Research on nonlinear behavior of link mechanism with clearance joint[J]. Journal of Machine Design, 2005, 22(03): 12-13.

[17]OLYAEI A A, GHAZAVI M R. Stabilizing slider-crank mechanism with clearance joints[J]. Mechanism & Machine Theory, 2012, 53(7): 17-29.

(责任编辑:李 磊)